

*Electronic Supplementary Information (ESI)*

# Photocatalytic oxidation surfaces on anatase TiO<sub>2</sub> crystal revealed by single-particle chemiluminescence imaging

Takashi Tachikawa\* and Tetsuro Majima\*

The Institute of Scientific and Industrial Research (SANKEN), Osaka University, Mihogaoka 8-1, Ibaraki, Osaka 567-0047, Japan

\*e-mail: tachi45@sanken.osaka-u.ac.jp (T.T.); majima@sanken.osaka-u.ac.jp (T.M.)

## Experimental methods

**Materials.** Tris(2,2'-bipyridyl)dichlororuthenium(II) hexahydrate and *cis*-bis(2,2'-bipyridyl)-(2,2'-bipyridyl-4,4'-dicarboxylic acid)ruthenium(II) hexafluorophosphate (named as Ruthenizer 455-PF6) were purchased from Aldrich and Solaronix, respectively, and used as received. Nanosized anatase TiO<sub>2</sub> particles (A-100, Ishihara Sangyo, 100–200-nm particles) were used as received. Microsized TiO<sub>2</sub> single crystals with dominant {001} and {010} facets were hydrothermally synthesized using titanium sulphate or titanium oxysulfate and hydrofluoric acid according to the procedure reported by Liu et al.<sup>S1,S2</sup> Crystallographic information and morphology of anatase TiO<sub>2</sub> single crystals were analyzed using powder X-ray diffraction (XRD) (Rigaku, RINT2500 XRD; Cu K $\alpha$  source) and scanning electron microscopy (SEM) (Hitachi, S-2150; an acceleration voltage of 25 kV), respectively.

**Instruments.** Steady-state UV–visible absorption spectra were measured with a UV–visible–NIR spectrophotometer (Shimadzu UV-3100). Steady-state fluorescence spectra were measured by a HORIBA FluoroMax-4 fluorescence spectrophotometer. All of the experimental data were obtained at room temperature.

**Sample preparation for single-particle chemiluminescence (CL) experiments.** The quartz cover glasses were purchased from DAICO MFG CO., Ltd. (Japan) and cleaned by sonication in a 20% detergent solution (As One, Cleanace) for 6 h, followed by repeated washings with warm running water for 30 min. Finally, the cover glasses were washed again with Milli-Q ultrapure water (Millipore). Well-dispersed aqueous suspensions of TiO<sub>2</sub> were spin-coated on the cleaned cover glasses. The cover glasses were annealed at 373 K for 1 h to immobilize the particles on the glass surface, and then mounted on the bottom of a stainless steel holder designed for viewing

specimens on the microscope. A cleaned cover glass was placed on the particle-coated glass using a 0.5-mm thickness Teflon spacer to form a chamber with an internal volume of about 150  $\mu\text{L}$ . An air-saturated sample solution was then introduced into this chamber and a cap with an O-ring seal was tightly screwed to prevent the solution from escaping. For the Ar-saturated samples, an Ar-saturated sample solution was introduced into the chamber in an Ar-purged glove box ( $[\text{O}_2] < 0.5 \text{ vol}\%$ ).<sup>S2</sup> The oxygen concentration was measured by an oxygen analyzer, maxO<sub>2</sub>+ (Maxtec, Inc.).

**Single-particle CL measurements with wide-field microscopy.** The experimental setup was based on an Olympus IX71 inverted fluorescence microscope. The position and size of the TiO<sub>2</sub> particles immobilized on the cover glass were determined by a transmission image obtained by illuminating the sample from above using a halogen lamp (Olympus, U-LH100L-3) and an atomic force microscope (AFM) image (Asylum Research, MFP-3DBIO), respectively. The 365-nm light emitted from an LED (OPTO-LINE, MS-LED-365) was reflected by a dichroic mirror (Olympus, DM455) and introduced to the sample through an ND filter and an objective (Olympus, UPLSAPO 100XO; 1.40 NA, 100 $\times$ ). The intensity of light passing through the objective, immersion oil, and cover glass was measured with a power meter (Ophir, Nova II) equipped with a PD300-UV head. For the 488 nm excitation, a light emitted from a CW diode laser (Coherent, CUBE 488-30FP) was reflected by a dichroic mirror (Olympus, DM505) and introduced to the sample.

The emission from the luminescent dyes generated over a single TiO<sub>2</sub> particle on the cover glass was collected using the same objective and passed through the dichroic mirror and two long-pass filters (Olympus, BA475 and Sigma Koki, SCF-50S-50Y) to remove the undesired scattered light, and then imaged by an electron-multiplying charge-coupled device (EM-CCD) camera (Roper Scientific, Cascade II:512). The images were recorded at a frame rate of 10 frames  $\text{s}^{-1}$  and processed using ImageJ (<http://rsb.info.nih.gov/ij/>) or OriginPro 8.1 (OriginLab). All experimental data were obtained at room temperature.

**Single-particle CL measurements with confocal microscopy.** Confocal fluorescence images were taken on an objective-scanning confocal microscope system (PicoQuant, MicroTime 200) coupled to an Olympus IX71 inverted fluorescence microscope. The samples were excited through an oil objective (Olympus, UPLSAPO 100XO; 1.40 NA, 100 $\times$ ) with a circular-polarized 380-nm pulsed laser (Spectra-Physics, MAI TAI HTS-W with an automated frequency doubler, Inspire Blue FAST-W; 0.8 MHz repetition rate, 1  $\mu\text{W}$  excitation power) controlled by a PDL-800B driver (PicoQuant). A circular-polarized 485-nm pulsed laser (PicoQuant, LDH-D-C-485; 20 MHz repetition rate, 1  $\mu\text{W}$  excitation power) was used to measure the emission lifetimes of the bulk solutions. The instrument response function (IRF) of  $\sim 100$  ps was obtained by measuring the scattered laser light in order to analyze the temporal profile. The emission was collected with the same objective and detected by a single photon avalanche photodiode (Micro Photon Devices, PDM 50CT) through a dichroic beam splitter (Chroma, z405/488rpc), long-pass filter (Chroma, HQ510LP), and 50- $\mu\text{m}$  pinhole for spatial filtering to reject out-of-focus signals. For spectrally resolved imaging, the emitted photons were separated into UV and visible regions by a half mirror and bandpass filters (Olympus, BP330-385 for UV and Semrock, FF01-609/152 for visible) and then detected by two detectors (Micro Photon Devices, PDM 50CT and PDM 100CT). The data collected using the PicoHarp 300 TCSPC module (PicoQuant) were stored in the time-tagged time-resolved mode (TTTR), recording every detected photon with its individual timing, which were used for the single-molecule analysis. All of the experimental data were obtained at room temperature.

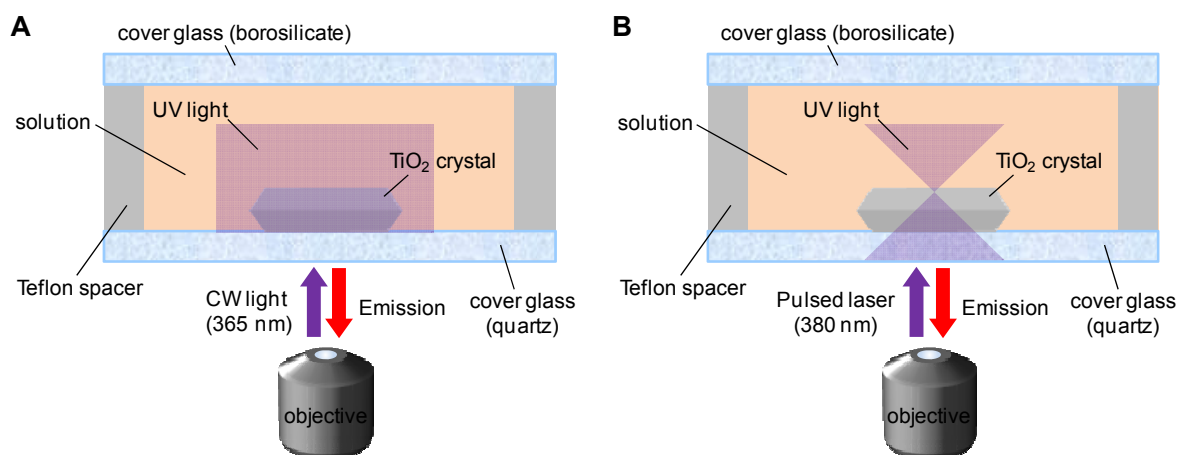


**Fig. S1.** Single-particle CL observations under epi (A) and confocal (B) illuminations. The solution in the chamber was exchanged with the other solutions of different concentrations. The CL images were captured under static conditions (i.e., without sample flow).

## Results and discussion

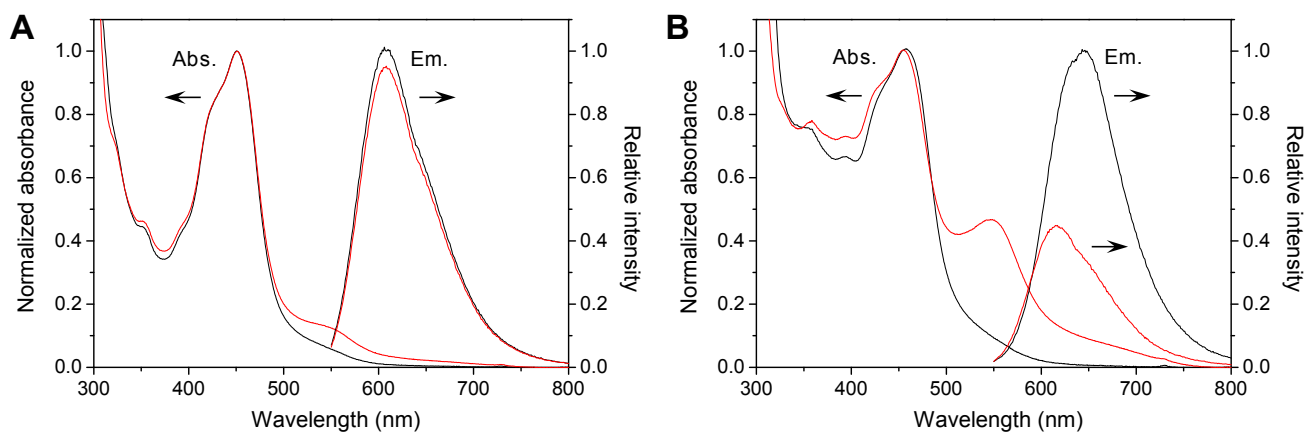


**Fig. S2.** Steady-state absorption and emission spectra of acetonitrile solutions of Ru(bpy)<sub>3</sub><sup>2+</sup> (0.1 mM) (A) and Ru(bpy)<sub>2</sub>(dcbpy)<sup>2+</sup> (0.1 mM) (B) in the absence (black lines) and presence (red lines) of TPA (0.1 M).

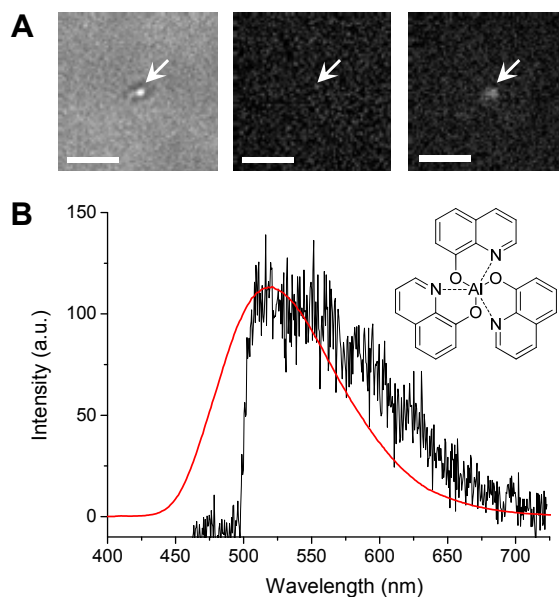


**Fig. S3.** (A) Transmission image (left) of a single TiO<sub>2</sub> nanoparticle or small aggregate on the cover glass and emission images of the same particle in acetonitrile solutions of Alq<sub>3</sub> (0.1 mM) in the absence (middle) and presence (right) of TPA (0.1 M) under 365-nm photoirradiation (500 mW cm<sup>-2</sup> at the glass surface). The scale bars are 2 μm. (B) Typical emission spectrum (black line) observed during 365-nm photoexcitation of a single TiO<sub>2</sub> nanoparticle in acetonitrile solution containing Alq<sub>3</sub> (0.1 mM) and TPA (0.1 M). The part of the spectrum (<500 nm) is cut off by the filters. The red line indicates the emission spectrum of the bulk acetonitrile solution containing Alq<sub>3</sub> (0.1 mM) and TPA (0.1 M) (excitation at 475 nm). The molecular structure of Alq<sub>3</sub> is also shown in the inset. The oxidation potential of Alq<sub>3</sub> is +1.4 V vs NHE.<sup>S3</sup> The CL intensity of the Alq<sub>3</sub>/TPA system is over an order of magnitude lower than those of the Ru dye/TPA systems. This tendency is similar to that reported by Richter et al. for the Al(HQS)<sub>3</sub> (HQS = 8-hydroxyquinoline-5-sulfonic acid)/TPA system.<sup>S4</sup>

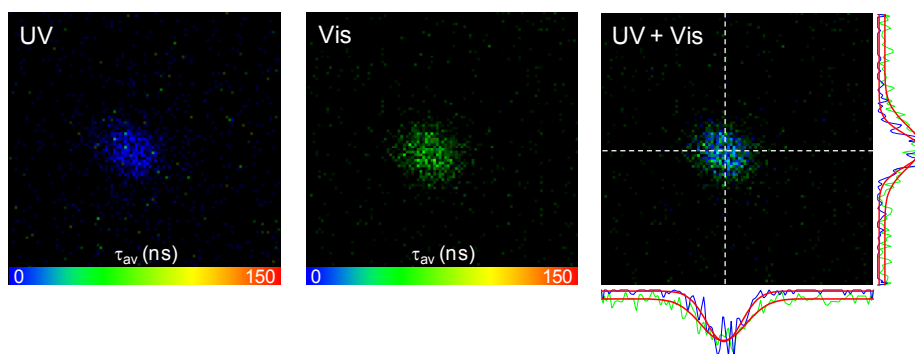


**Fig. S4.** (A) Emission lifetime images acquired under 380-nm pulsed laser irradiation of a single TiO<sub>2</sub> nanoparticle in acetonitrile solution containing Ru(bpy)<sub>2</sub>(dcbpy)<sup>2+</sup> (0.1 mM) and TPA (0.1 M). The emitted photons were separated into UV (left) and visible (middle) regions by using a half mirror and bandpass filters and were then detected by two detectors. The merged image is also shown on the right. The red lines indicate the Gaussian fitting to the line profiles (see dashed lines) of the emission intensity in UV (blue) and visible (green) regions. These images are spatially coincident and the full width at half maxima of the luminescent spots were determined to be about 280 and 380 nm for light scattering and dye emission, respectively, which approximate those of diffraction limited spots at corresponding wavelengths.

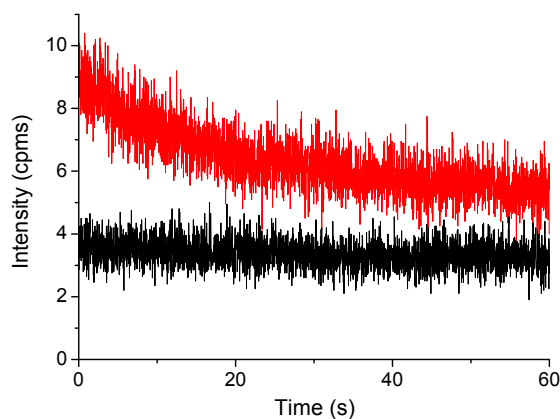


**Fig. S5.** Typical time trajectories of the CL intensity observed for single TiO<sub>2</sub> particles.

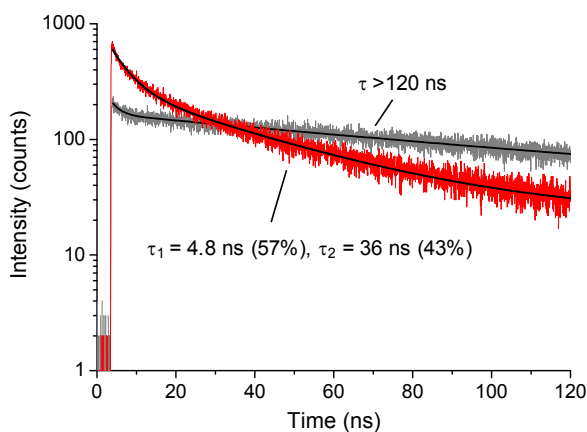


**Fig. S6.** Emission decay profile (red line) recorded for a single TiO<sub>2</sub> nanoparticle in acetonitrile solution containing Ru(bpy)<sub>2</sub>(dcbpy)<sup>2+</sup> (0.1 mM) and TPA (0.1 M). The gray line indicates the emission decay profile observed during 485-nm pulsed laser excitation of Ru(bpy)<sub>2</sub>(dcbpy)<sup>2+</sup> (0.1 mM) in acetonitrile. Black lines indicate double-exponential curves fitted to the data. The lifetime of Ru(bpy)<sub>2</sub>(dcbpy)<sup>2+</sup> is too long to be measured accurately on the time scale of this experiment, but was reported as 490 ns and 180 ns for degassed and aerated acetonitrile solutions, respectively.<sup>S5</sup> The slight deviation from exponential behavior observed at short times might be attributed to the clustering of the dye molecules with resultant excited state annihilation. Ruthenium dyes and TPA are both adsorbed on the TiO<sub>2</sub> surface before laser irradiation (Fig. 1D). It is likely that interfacial hole transfer from the excited TiO<sub>2</sub> to adsorbed molecules occurs in femto-to-picosecond time range.<sup>S6</sup> This time scale is much shorter than the time resolution of our detection system (ca. 100 ps). Furthermore, the surface chemical reactions are heterogeneous in nature, resulting in a broad distribution of reaction rates.<sup>S7</sup> In addition to this heterogeneity, the undesired background signal (ca. 20% of detected photons) from free dye molecules in the bulk solution makes it difficult to resolve the dynamic processes involved in the CL mechanism.

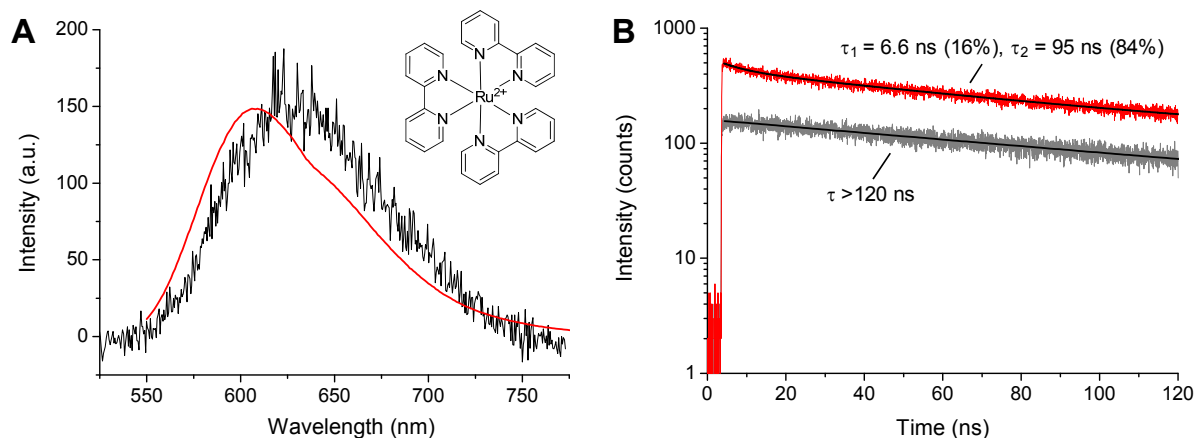


**Fig. S7.** (A) Typical emission spectrum (black line) observed during 365-nm photoexcitation of a single TiO<sub>2</sub> nanoparticle in acetonitrile solution containing Ru(bpy)<sub>3</sub><sup>2+</sup> (0.1 mM) and TPA (0.1 M). The red line indicates the emission spectrum of the bulk acetonitrile solution containing Ru(bpy)<sub>3</sub><sup>2+</sup> (0.1 mM) and TPA (0.1 M) (excitation at 475 nm). The molecular structure of Ru(bpy)<sub>3</sub><sup>2+</sup> is also shown in the inset. (B) Emission decay profile (red line) observed during 380-nm pulsed laser excitation of a single TiO<sub>2</sub> nanoparticle in acetonitrile solution containing Ru(bpy)<sub>3</sub><sup>2+</sup> (0.1 mM) and TPA (0.1 M). The gray line indicates the emission decay profile observed during 485-nm pulsed laser excitation of Ru(bpy)<sub>3</sub><sup>2+</sup> (0.1 mM) in acetonitrile. Black lines indicate single- or double-exponential curves fitted to the data.

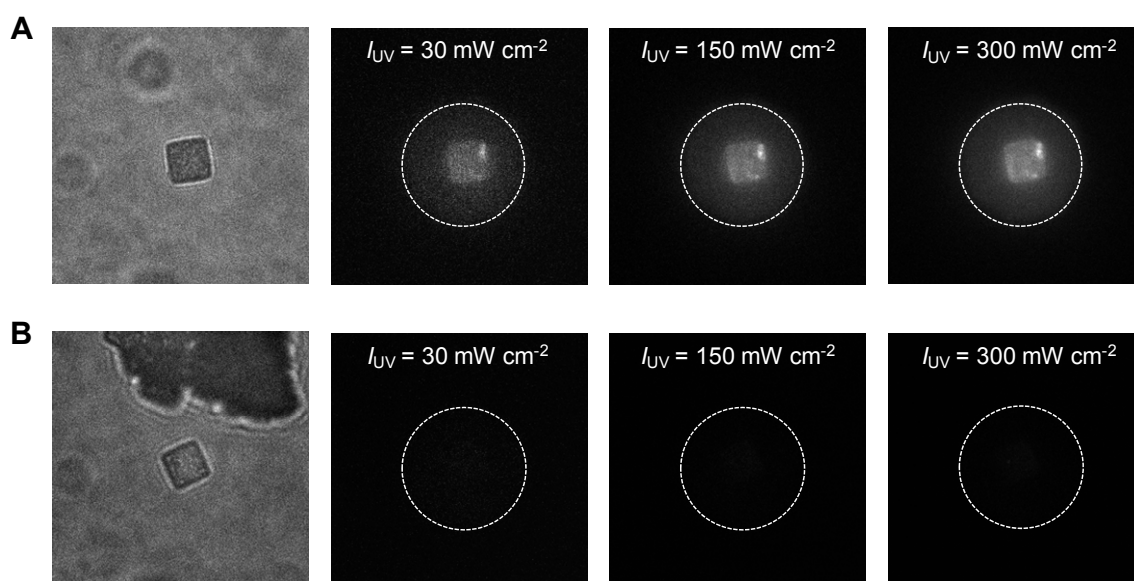


**Fig. S8.** Transmission and emission images of TiO<sub>2</sub>{001} crystals in acetonitrile solution of Ru(bpy)<sub>3</sub><sup>2+</sup> (0.1 mM) in the presence (A) and absence (B) of TPA (0.1 M) under 365-nm photoirradiation. The emission intensity thresholds are the same for images observed at same UV intensities. The UV irradiation area is inside the white circle in the images. The image size is 25 μm × 25 μm. The CL intensities are almost uniformly distributed over the crystal. In addition, no significant contribution from light scattering was observed.

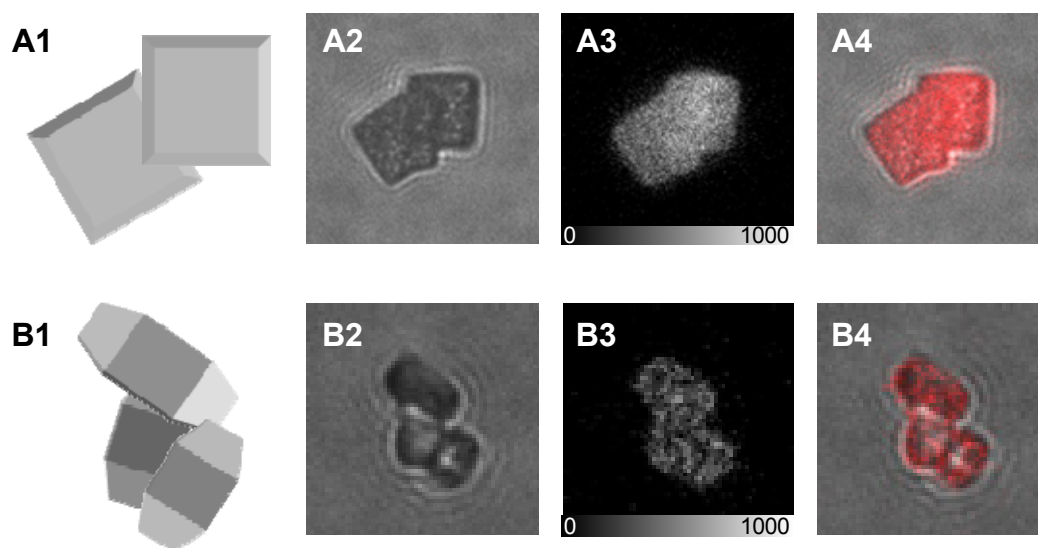


**Fig. S9.** Spatial analysis of the photocatalytic oxidation sites on individual anatase  $\text{TiO}_2$  crystals. (A1) Illustration of attached  $\text{TiO}_2$  crystals with dominant  $\{001\}$  facets ( $\text{TiO}_2\{001\}$ ). Transmission (A2) and emission (A3) images of  $\text{TiO}_2\{001\}$  crystals in solution under 365-nm photoirradiation. The merged image of transmission (gray) and emission (red) is also shown (A4). (B1) Illustration of attached  $\text{TiO}_2$  crystals with dominant  $\{010\}$  facets ( $\text{TiO}_2\{010\}$ ). Transmission (B2) and emission (B3) images of  $\text{TiO}_2\{010\}$  crystals in solution under 365-nm photoirradiation. The merged image of transmission (gray) and emission (red) is also shown (B4). All acetonitrile solutions contain  $\text{Ru}(\text{bpy})_2(\text{dcbpy})^{2+}$  (0.1 mM) and TPA (0.1 M). The numbers in images A3 and B3 are emission intensity in counts.

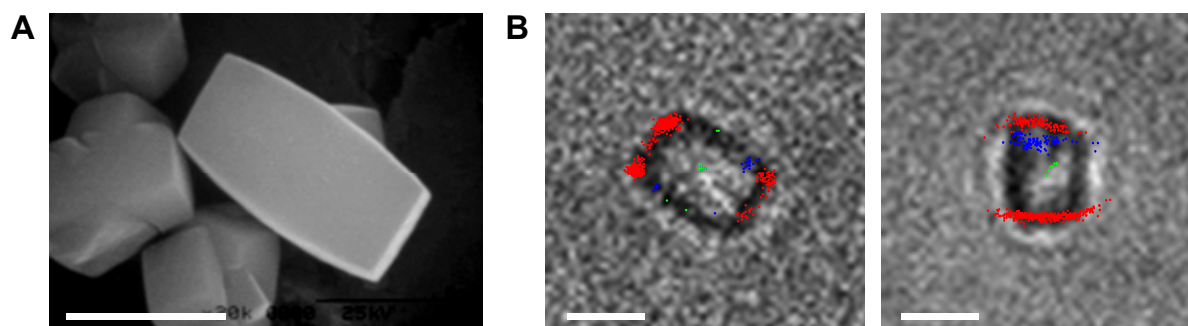


**Fig. S10.** (A) SEM image of synthesized  $\text{TiO}_2\{010\}$  crystals. (B) Transmission (middle and right) images of  $\text{TiO}_2\{010\}$  crystals on the cover glass in Ar-saturated methanol solutions of 3,4-dinitrophenyl-BODIPY (DN-BODIPY) ( $2\ \mu\text{m}$ ). The red, blue, and green dots in images indicate the fluorescence bursts located on the  $\{101\}$ ,  $\{001\}$ , and  $\{010\}$  surfaces, respectively, observed during 3-min irradiation. The precise positions at which fluorescent products were generated were determined by centroid analysis. See ref. S2 for details of the experimental and analytical procedures. The scale bars are  $2\ \mu\text{m}$ .

## References

- S1 (a) J. Pan, G. Liu, G. Q. (Max) Lu and H.-M. Cheng, *Angew. Chem. Int. Ed.*, 2011, **50**, 2133; (b) T. Tachikawa, N. Wang, S. Yamashita, S.-C. Cui and T. Majima, *Angew. Chem. Int. Ed.*, 2010, **49**, 8593.
- S2 T. Tachikawa, S. Yamashita and T. Majima, *J. Am. Chem. Soc.*, 2011, **133**, 7197.
- S3 T. D. M. Bell, C. Pagba, M. Myahkostupov, J. Hofkens and P. Piotrowiak, *J. Phys. Chem. B*, 2006, **110**, 25314.
- S4 T. Tachikawa, S. Tojo, M. Fujitsuka and T. Majima, *Chem. Eur. J.*, 2006, **12**, 7585
- S5 J. D. Anderson, E. M. McDonald, P. A. Lee, M. L. Anderson, E. L. Ritchie, H. K. Hall, T. Hopkins, E. A. Mash, J. Wang, A. Padias, S. Thayumanavan, S. Barlow, S. R. Marder, G. E. Jabbour, S. Shaheen, B. Kippelen, N. Peyghambarian, R. M. Wightman and N. R. Armstrong, *J. Am. Chem. Soc.*, 1998, **120**, 9646-9655.
- S6 B. D. Muegge, S. Brooks and M. M. Richter, *Anal. Chem.*, 2003, **75**, 1102.
- S7 T. Tachikawa and T. Majima, *Chem. Soc. Rev.*, 2010, **39**, 4802.